JACS
JOURNAL OF THE AMERICAN CHEMICAL SOCIETY

ARTICLE

pubs.acs.org/JACS

Cations Strongly Reduce Electron-Hopping Rates in Aqueous Solutions

Niklas Ottosson,[*,†] Michael Odelius,[*,‡] Daniel Spångberg,[*,§] Wandared Pokapanich,[†] Mattias Svanqvist,[⊥] Gunnar Öhrwall,[∥] Bernd Winter,[#] and Olle Björneholm[†]

[†]Department of Physics and Astronomy, Uppsala University, Box 516, SE-751 20 Uppsala, Sweden

[‡]Fysikum, Albanova University Center, Stockholm University, SE-106 91 Stockholm, Sweden

[§]Department of Materials Chemistry, Uppsala University, Box 538, SE-751 21 Uppsala, Sweden

[⊥]Fakultät für Physik, Universität Freiburg, Stefan-Meier Strasse 19, D-79104 Freiburg, Germany

[∥]MAX-lab, Lund University, Box 118, SE-221 00 Lund, Sweden

[#]Helmholtz-Zentrum Berlin für Materialien und Energie, and BESSY, Albert-Einstein-Strasse 15, D-12489 Berlin, Germany

Supporting Information

ABSTRACT: We study how the ultrafast intermolecular hopping of electrons excited from the water O1s core level into unoccupied orbitals depends on the local molecular environment in liquid water. Our probe is the resonant Auger decay of the water O1s core hole (lifetime ∼3.6 fs), by which we show that the electron-hopping rate can be significantly reduced when a first-shell water molecule is replaced by an atomic ion. Decays resulting from excitations at the O1s post-edge feature (∼540 eV) of 6 *m* LiBr and 3 *m* $MgBr_2$ aqueous solutions reveal electron-hopping times of ∼1.5 and 1.9 fs, respectively; the latter represents a 4-fold increase compared to the corresponding value in neat water. The slower electron-hopping in electrolytes, which shows a strong dependence on the charge of the cations, can be explained by ion-induced reduction of water−water orbital mixing. Density functional theory electronic structure calculations of solvation geometries obtained from molecular dynamics simulations reveal that this phenomenon largely arises from electrostatic perturbations of the solvating water molecules by the solvated ions. Our results demonstrate that it is possible to deliberately manipulate the rate of charge transfer via electron-hopping in aqueous media.

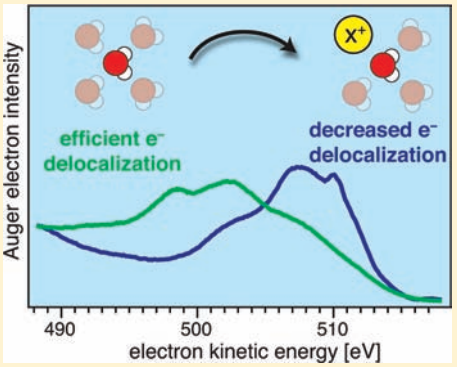

1. INTRODUCTION

Charge-transfer phenomena in aqueous environments are essential for numerous chemical and biochemical as well as technological processes and applications.[1] While charge-transfer rates in the electronic ground state of most redox systems are relatively well described by standard Marcus theory,[2] there lies great interest in improving models for charge transfer between neighboring sites initiated by photoinduced electronic transitions in solution. For example, such processes play a key role in the function of electrolyte-based dye-sensitized solar cells.[3] In most cases, the solvent is considered to only passively assist such processes, e.g., by enabling the redox couple to interact in favorable geometries, and is therefore not really involved in the charge transfer *per se*. Nevertheless, there exist several charge-transfer phenomena where the solvent molecules play a much more active role, such as charge-transfer-to-solvent (CTTS) absorption processes[4] and solvent-mediated proton-transfer reactions, which are ubiquitous in aqueous environments.[5]

One important mechanism for charge transfer is electron-hopping, which for liquid water has recently been reported to extend down to attosecond time scales upon resonant excitation of a core electron into unoccupied orbitals.[6] The ultrafast time scale makes these processes extremely challenging to study experimentally directly in the time domain, and an attractive alternative is to use the short lifetime associated with the decay of the O 1s core hole (∼3.6 fs) itself to indirectly probe the concurrent ultrafast electron-hopping. The dynamical information can be accessed by analysis of the different channels in the associated Auger electron spectra, which reflect whether the excited electron has left the initial excitation site during the core-hole lifetime.[7] The principle is schematically illustrated in Figure 1, showing the relevant electronic decay processes of core-ionized/core-excited molecules. On a microscopic scale, the rate of electron-hopping depends on both the spatial and energetic overlap between the orbital into which the electron has been excited and the empty orbitals of the neighboring molecules. Due to the locally disordered nature of liquids, this is not as easily defined as in crystalline systems, for which hopping rates can be connected to bandwidth. Locally, however, the hopping rates in liquid water are determined by the same basic mechanisms.[8]

Received: May 4, 2011
Published: July 14, 2011

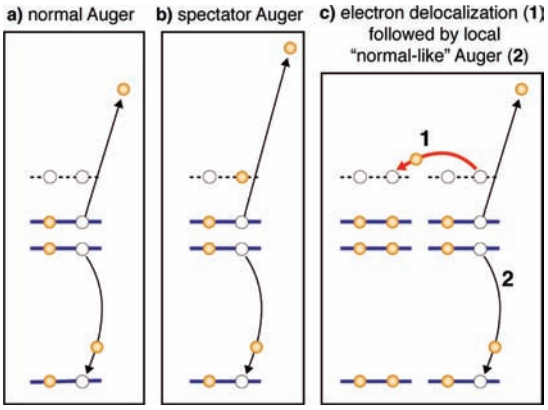

Figure 1. Schematic electronic-level diagram illustrating how different autoionization pathways of a core-ionized/core-excited molecule in solution can be used to identify ultrafast charge-transfer mechanisms. (a) The normal Auger process. The core hole of a core-ionized molecule is refilled by a valence electron, causing the ejection of another valence electron and leaving the system in a doubly ionized state. (b) The most probable decay channel from a molecule, where the initial excitation does not lead to ionization but instead promotes a core electron to an initially unoccupied energy level (dashed line). The Auger decay now occurs in the presence of the excited electron, and hence the final state will be different from that shown in (a), due to the screening of the excited electron. This process is referred to as spectator Auger decay. (c) The situation where a resonantly excited molecule (to the right) quickly donates the excited electron to a neighboring molecule through charge transfer (labeled 1), prior to the decay of the core hole. The subsequent autoionization process will thus locally look like a normal Auger decay (labeled 2). If the delocalization and core-hole decay rates are comparable, the Auger spectra upon resonant excitation will contain both spectator and "normal-like" contributions. From their relative intensities together with the core-hole lifetime, the delocalization time scale and rate can be deduced.

In this work we demonstrate that the addition of simple inorganic salts strongly slows down the ultrafast electron delocalization from a resonantly core-excited water molecule into the H-bonding network. Even though we cannot experimentally fully disentangle the effects of anions and cations, comparison between solutions of different salts reveals that the magnitude of the effect depends strongly on the cationic charge. Further insight into the microscopic mechanism is given by molecular dynamics (MD) simulations and electronic structure calculations using density functional theory. On the basis of our findings, we propose a qualitative model in which the resonantly excited electron is "back-polarized" toward the parental core-excited water molecule when engaged in cation solvation. This reduces the electronic overlap with other neighboring molecules in the excited state, slowing down the ultrafast delocalization dynamics observed in pure water.

2. METHODS

2.1. Experimental Section. O1s resonant Auger spectra of liquid water as well as of 6 *m* LiBr and 3 *m* $MgBr_2$ aqueous solutions were recorded at the U-41 PGM microfocus undulator beamline at the BESSY synchrotron facility, Berlin, Germany, which delivers soft X-ray photons in the 180−1500 eV range. The experimental setup has previously been described in detail.[9,10] Briefly, the liquid samples are injected into the evacuated experimental chamber as a 15 μm jet, traveling at a velocity of ∼100 m/s. The liquid jet propagates in the plane of the linearly polarized synchrotron radiation and is perpendicular to the detection axis of the hemispherical electron analyzer. The expelled electron enters the analyzer through a circular opening with a diameter of 0.2 mm, situated 0.5 mm from the liquid surface. Such an arrangement allows for good differential pumping of the spectrometer (at $\sim 10^{-8}$ mbar) while a sufficiently small fraction of the photoelectrons is lost in the short passage through the vapor. Further, the favorable overlap between the synchrotron focal spot at the U-41 PGM beamline ($23 \times 12\ \mu m^2$) and the liquid microjet results in negligible gas-phase contributions to the spectra.

All samples were prepared from highly demineralized water. Salts were purchased from Sigma-Aldrich and were used without further purification (LiBr > 99.9% and $MgBr_2$ > 99.8%).

2.2. Molecular Dynamics Simulations. Classical MD simulations were performed for LiBr(aq) and $MgBr_2$(aq), as well as for pure water. For the salt solutions, systems of two different sizes were used. For LiBr(aq), the large system contained 1512 water molecules, 162 Li^+, and 162 Br^- ions, while the small system contained 76 water molecules, 8 Li^+, and 8 Br^- ions. For $MgBr_2$(aq), the large system contained 1512 water molecules, 81 Mg^{2+}, and 162 Br^- ions, while the small system contained 76 water molecules, 4 Mg^{2+}, and 8 Br^- ions. The pure water simulation contained 1024 water molecules. The SPC/E water model was used in all cases.[11] The Li^+ and Br^- ions were described by the ion−water Lennard-Jones parameters of Horinek et al.[12] Lorenz−Berthelot combination rules were used to derive the Li^+−Li^+, Br^-−Br^-, and Li^+−Br^- Lennard-Jones interactions. The Mg^{2+}−water potentials used were the three-body potentials of Spångberg and Hermansson,[13] while the Mg^{2+}−Mg^{2+} and Mg^{2+}−Br^- interactions were derived using Lorenz−Berthelot combination rules from the Mg^{2+}−water Lennard-Jones parameters of Åqvist.[14] Standard cubic periodic boundary conditions were used, with short-range interactions truncated using a spherical cutoff distance of 13 Å for the pair interactions and an ion−oxygen distance of 6 Å for the three-body interactions in the Mg^{2+}−water potential. Ewald lattice sums were used for the Coulomb interactions.[15] The temperature was set to 300 K and the pressure to 0 Pa using Nosé−Hoover extended system dynamics[16,17] to obtain the NPT ensemble. The water molecules were kept rigid using the RATTLE algorithm[18] with successive over-relaxation to increase the speed of convergence.[19] The equations of motion were integrated with the velocity Verlet integrator[20] employing a time step of 1.5 fs.

The starting positions and angles for the species in the LiBr(aq) simulations were selected randomly on a primitive cubic lattice, while for the $MgBr_2$(aq) simulations, it was ensured that each Mg^{2+} ion was surrounded by six water molecules initially, since the mean residence time of water molecules in the first solvation shell of Mg^{2+} is about 1 ms,[21] substantially longer than the possible time scale for the simulations. Thus, should the initial configuration of the simulation contain bromide ions in the first solvation sphere of magnesium ions, a long time might be required to displace the bromide ions by water molecules. The simulations were equilibrated for 300 ps, followed by 1.2 ns of production. The obtained average volumes for the small and large LiBr(aq) simulations were 2776 and 55 315 $Å^3$, respectively, while for the small and large $MgBr_2$(aq) simulations the volumes were 2576 and 47 500 $Å^3$, respectively. The concentrations of the salt solutions are thus 4.8 and 4.9 M for the small and large LiBr(aq) simulations, respectively. The corresponding values for the small and large $MgBr_2$(aq) simulations are 2.6 and 2.8 M.

2.3. Electronic Structure Calculations. We have investigated the electronic structure in single snapshots from the small classical MD simulations with 76 water molecules in concentrated LiBr(aq) and $MgBr_2$(aq) solutions to guide the interpretation of the experimental spectra. The partial density of states (PDOS) in the ground state is derived to resolve the chemical bonding and mixing of the states in electrolyte solution.

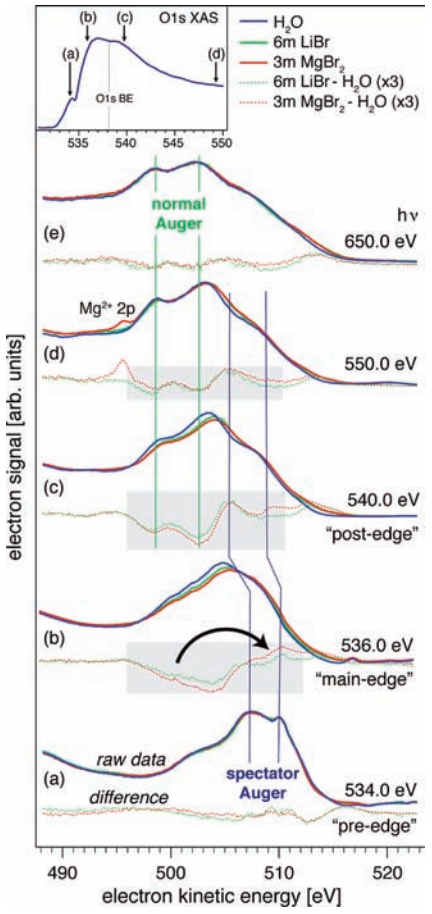

Figure 2. O1s resonant/off-resonant Auger spectra of liquid water and 6 *m* LiBr/3 *m* $MgBr_2$ aqueous solutions. The inset (top left) shows the excitation energies, projected onto the water X-ray absorption spectrum. The dotted lines under each trace are the difference spectra of the respective solution minus water at the given photon energy. The gray boxes in the difference spectra of traces (b) and (c) highlight a characteristic spectral redistribution at the main and post edges discussed in the main text.

Electronic structure calculations performed in the density functional framework of the CPMD code[22] were used to derive PDOS and X-ray absorption spectra (XAS) as previously implemented.[23−25] The gradient-corrected density functional BLYP[26,27] was used. The calculations in CPMD employed pseudopotentials in combination with an 85 Ry kinetic energy (KE) plane-wave cutoff in the expansion of the Kohn−Sham wave functions. To cover the spectral region of interest, a large number of unoccupied orbitals was required, and 800 Kohn−Sham states were calculated in each system. A Troullier−Martins-type pseudopotential[28] expressed in the Kleinman−Bylander form[29] was used for bromine. The cations were described by Goedecker pseudopotentials.[30,31]

We calculate averages for different environments to investigate how the electronic structure varies locally in the electrolyte. By transforming the intensities into the molecular frame[32] before averaging, we obtain a comprehensive picture of the chemical bonding in terms of the symmetry classes of the isolated water molecule. The b_1 component is perpendicular to the molecular plane, the a_1 component is along the molecular axis, and the b_2 component is their cross-product, approximately along the intramolecular H−H direction.

3. RESULTS AND DISCUSSION

Figure 2 shows a series of Auger spectra in the 488−523 eV KE range, obtained from pure liquid water, 6 *m* LiBr, and 3 *m* $MgBr_2$ (i.e., with equal Br^- concentrations) at varying excitation energies. The top-left inset shows XAS of liquid water with labeled arrows (a−d) that indicate the choice of photon energies used to obtain the associated Auger spectra. The three lowest energies correspond to excitations into the three main features of the water XAS; in the following we will adopt the terminology of Wernet et al. and refer to these as the pre- (a), main- (b), and post-edge (c), respectively.[33] Most important for the present study is that excitations into successively higher core-excited states lead to distinguishable spectator shifts in resonant absorption spectroscopy (RAS) as a function of photon energy throughout the near-edge absorption fine structure.[34] This behavior implies a persistent excitonic particle−hole interaction in the core-excited states, which induces a localization of the excited electron at the core-excited molecule during the core-hole lifetime.[35,36]

As we are interested in ion-induced effects, each trace in Figure 2 shows difference spectra formed from the respective solution spectra minus that of water at the same photon energy (magnified by a factor 3 for better visibility). In the following we go through the electronic decay spectra associated with each of the excitations. We first consider the simpler cases of the lowest and highest photon energies, (a) and (e), before we proceed with the more complex and intriguing intermediate cases, (b)−(d).

At the pre-edge resonance (a), we observe a pronounced spectator shift of ∼5 eV to higher KE relative to off-resonance excitations. This has previously been interpreted as a fingerprint of a high degree of localization of the excited electron.[6,34] We here make the observation that the spectra of electrolyte solutions look nearly identical to that of the pure water reference. This is a strong indication that the localization in the corresponding core excitations is not substantially affected by solvated ions. Even though the molecular environment is typically quite different in the two cases, the core hole of an excited water molecule is similarly screened, and the resulting spectator spectra are therefore very similar.

Trace (e) is taken at 650 eV photon energy and is therefore clearly off-resonant, the O1s BE of liquid water being 538.1 eV.[37] We again note that the solution spectra and the water reference look nearly identical. Even though *ab initio* electronic structure calculations have shown that water molecules residing in the first solvation shell of solvated ions display significant polarization (gradually increasing with charge from monovalent to trivalent species),[38] we have recently demonstrated that the only clear effect of ions on the off-resonance O1s Auger spectrum of liquid water is limited to the high-energy region (507−515 eV KE), pertaining to various delocalized two-hole final states.[39] Briefly, the positive features around 514 eV KE in the difference spectra of trace (e) originate from bromide−water double-hole final states. In a similar fashion, the decrease centered around 510 eV originates from a reduced number of water−water delocalized final states due to H-bonding interactions, a relaxation channel that has been discussed in great detail elsewhere.[40] While this striking overall insensitivity in the off-resonance Auger spectra to ion-induced electronic structure modification may at first seem disappointing, this actually simplifies the interpretation of the resonant Auger spectra (a−c) considerably.

Turning to the decay spectra associated with resonant excitation in the main-edge region (b), we start to observe pronounced differences between the solution spectra and the water reference. These differences become even more pronounced at the post-edge (c) and gradually diminish at higher excitation energies; gray boxes in Figure 2 highlight the important regions. In all cases

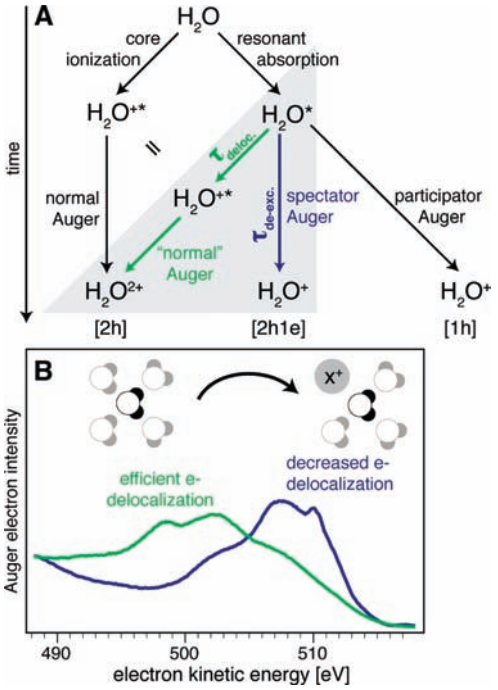

Figure 3. (A) Schematic flow diagram showing how different final states can be reached through Auger decay after O1s core ionization/resonant absorption of a water molecule in the aqueous phase. The core-ionized H_2O^{+*} state can solely decay through normal Auger decay (left branch). Resonant absorption (right branch), however, produces a wide range of intermediate states, whose nature depends on the excitation energy. Depending on the efficiency for delocalization of the electron in the excited state (characterized by the lifetime τ_{deloc}), either a doubly charged [2h] cationic state or a singly charged valence-exited [2h1e] state is reached, each with a distinct signature in the resulting Auger spectrum. Since the core-hole lifetime (here denoted $\tau_{de\text{-}exc}$) is known (3.6 fs), the delocalization time τ_{deloc} can be derived by analysis of the spectral branching ratio. (B) Conceptual illustration of how ion coordination of a resonantly excited molecule reduces the delocalization rate during the core-hole lifetime, and how this is reflected in the final Auger spectrum.

we see intensity redistribution (indicated by the arrow) from a region centered around 500 eV to a band at higher KEs, which moves to lower energies upon going from main- to post-edge excitations.

As indicated by the vertical lines in Figure 2, the high KE region is associated with spectator Auger decays, where a neutral core-excited water molecule (H_2O^*) is transformed to an excited, singly valence-ionized H_2O^+. As previously mentioned, these Auger transitions lie at high KEs due to the screening of the core hole by the resonantly excited electron and signify that it remained localized on its parent molecule until the decay occurred. We note that the difference with respect to pure water is strongest for post-edge core excitations but is also present at higher energies, indicating an influence from resonances even at 550 eV.

The XAS of liquid water is strongly influenced by H-bonding, and the main- and post-edge features are due to resonances from valence excitations in the conduction band.[41] The presence of resonances in the continuum will induce a localization of the core-excited electron, and as a result the resonant Auger spectra deviate from the normal Auger spectrum. As expected, the spectator features decrease in KE with increasing excitation energy, as the screening efficiency of the excited electron decreases for higher, and spatially more extended, intermediate states. In contrast, the low KE region originates from normal Auger decays, i.e., a transition from the singly core-ionized H_2O^{+*} to the double valence-ionized H_2O^{2+}, meaning that the electron has delocalized prior to the core-hole decay. This means that the intermediate state has lost its "memory" of the initial excitation, and the final state KE is independent of excitation energy.

The differences in localization of the excited electron between pure water and the ionic solutions revealed by the features in the difference spectra unambiguously show that the introduction of ions into the H-bonding network of liquid water changes the electron delocalization times in the excited states. Since the fraction of Auger decays where the excited electron remains localized is larger with ions than without, we conclude that the ions slow down the electron delocalization dynamics. Figure 3 illustrates this picture in some further detail: Core ionization (left branch) produces a H_2O^{+*} state where the electron has instantaneously been delocalized, due to the sudden nature of the photoionization process.[42] There is then no other electronic decay path available except for normal Auger decay, leading to a variety of H_2O^{2+} two-hole final states. The possibilities become more diverse upon resonant core excitation (right branch in Figure 3), producing neutral H_2O^* intermediate states. For completeness, we have included the participator Auger channel to the far right in Figure 3, in which the excited electron has participated in the decay. However, these states overlap with the direct valence photoemission features and lie outside the KE window considered here. Furthermore, these features are very weak compared to the spectator contributions. For the present discussion we are therefore concerned with the branching ratio between the spectator channel producing H_2O^+ (two hole-one electron) final states and the doubly ionized states reached via the intermediate core-ionized state through ultrafast delocalization of the excited electron into the H-bonded surroundings. The latter closely resembles the mechanism of "internal ionization" observed for similar excitations in other nonmetallic systems.[43] The channels of main interest are marked with a gray triangle in Figure 3.

O1s XAS has previously been applied to aqueous electrolyte solutions in several studies.[44−47] The ion-induced variations in the XAS have been analyzed primarily in terms of either changes in local electronic structure on the solvating water molecules or H-bonding effects. The present study of the resonant Auger decay of the core-excited states is naturally linked to the XAS data and can contribute to our understanding of the XAS features and the electronic structure of electrolyte solution. Cappa et al. have reported XAS from aqueous solutions of divalent cations (including Mg^{2+}), showing considerably more structure in the main- and post-edge regions compared to that of pure water. This was interpreted to arise due to the strong electrostatic perturbation of the cations on the solvating water molecules.[45] This fits well with the picture emerging from the current experiments, as 3 *m* $MgBr_2$ leads to stronger RAS difference features at these resonances than 6 *m* LiBr, suggesting that the electron delocalization rates are highly dependent on the nature of the solvated cation. The higher degree of structure in the solution XAS also signifies the presence of resonances farther up in the continuum, which could explain why we see a weak effect of ion-induced electron localization as high as 550 eV excitation energy, whereas the normal Auger contribution totally dominates for pure water at this energy.

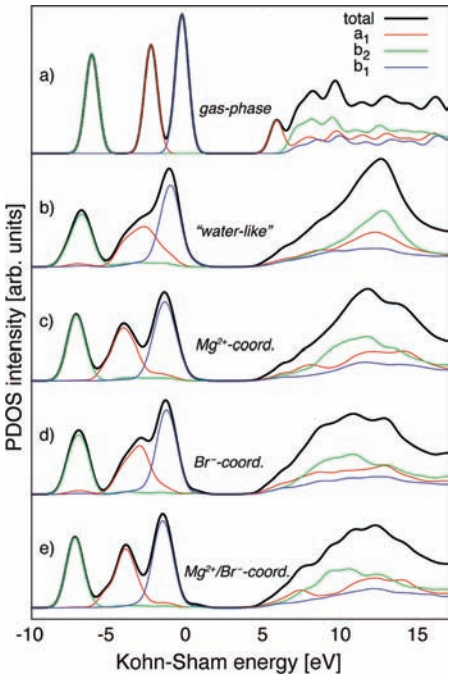

Figure 4. Calculated occupied and unoccupied density of states of p-character (PDOS) for (a) the water molecule in the gas phase and (b−e) different classes of water molecules from MD simulations of ∼3 *m* $MgBr_2$: (b) "water-like" water, i.e., those which only coordinate to other water molecules, (c) those which coordinate to at least one Mg^{2+}, (d) those which coordinate to at least one Br^-, and (e) those which coordinate to both $Mg^{2+}$and Br^-.

If a reliable decomposition of the resonant spectra in Figure 2 could be made, we could apply the "core-hole clock" method to obtain a value of τ_{deloc} for the respective excitations of each solution.[7] In practice this is challenging, given that we do not have access to the isolated spectator spectrum at higher excitation energies. If we knew the respective spectator and normal Auger fractions in the corresponding pure water spectra, however, we could estimate the changes in delocalization time on the basis of the respective difference spectra in Figure 2; details on how to estimate this are given in the Supporting Information (SI). Assuming τ_{deloc} = 0.5 fs for post-edge excitation in pure water, as reported in ref 6, we can in this way determine the corresponding values in 6 *m* LiBr and 3 *m* $MgBr_2$ to be ∼1.5 and 1.9 fs, respectively, meaning that the ions slow down the hopping rate by almost 400% in the latter case. Note that this value is an ensemble average and that molecules in different binding environments may well contribute to very different extents. Since the value of τ_{deloc} for main-edge excitation of pure water has not been reported (and cannot be accurately determined in the present study), it is not possible to make the corresponding estimation for the ion-induced reduction of the electron-hopping rate at this resonance. The reason the large ion-induced variations in electron-hopping times upon post-edge excitation lead to rather small spectral changes (Figure 2c) is the nonlinear relationship between lifetime variations and corresponding changes in spectral intensity, an inherent property of the core-hole clock method.[7]

In order to rationalize the experimental findings in terms of molecular and electronic structure and to separate various contributions to the ion-induced changes in electron delocalization times, we have calculated occupied and unoccupied electronic density of states of p-character (PDOS) from the MD simulations as described in sections 2.2 and 2.3. The differences in structures obtained from the large and small classical MD simulations are small, validating the use of the small simulations in the electronic structure calculations (see the SI for details). We limit the analysis to the oxygen p-character, which can be related to the transition probabilities for core excitations. We are especially interested in identifying which intermolecular configurations primarily contribute to the spectral redistribution observed upon main- and post-edge excitations in Figure 2. Therefore, the water molecules from each MD snapshot have been divided into discrete classes of environments on the basis of their ion coordination and H-bonding configuration; details on the criteria and the resulting H-bonding statistics are given in the SI. While as many as 187 discrete classes can be identified, they fall naturally into four main categories:

(1) those which are "water-like", i.e., only coordinate to other water molecules
(2) those which coordinate to at least one Mg^{2+} cation
(3) those which coordinate to at least one Br^- anion
(4) those which coordinate to both Mg^{2+} and Br^- ions

Figure 4 shows the calculated PDOS for these four categories (b−e) together with that for the H_2O monomer in the gas phase (a). The black lines show the total PDOS, while the red, green, and blue components reveal the respective contributions of a_1, b_2, and b_1 symmetry, respectively. Local p-character in each orbital is projected onto the axes in the molecular frame, which allows for symmetry decomposition of the PDOS. This analysis is motivated by the clear symmetry separation of the features in the occupied PDOS. Relative to the occupied orbitals, the larger spatial extension of the unoccupied orbitals makes them more sensitive to a mixing of states due to symmetry-breaking intermolecular interactions, in particular H-bonding, and the analysis has to be performed with caution. However, when this is applied, we observe systematic trends in the symmetry-decomposed unoccupied PDOS which are naturally correlated with the changes in the occupied orbitals. Hence, we conclude that symmetry analysis is a valuable tool to resolve changes in the electronic structure, which is contained in the total PDOS.

By comparing traces (a) and (b), we see that the H-bonding in the condensed phase causes a significant broadening of all electronic states. Importantly, the $3a_1$ orbital in the occupied DOS, which is engaged in forming the intramolecular O−H bond, is known to mix with neighboring water molecules upon H-bonding due to the spatial and energetic overlap of the $3a_1$ orbitals.[24] This causes the characteristic splitting into bonding and antibonding components, seen around −5 to −1 eV in trace (b) of Figure 4. Note that this phenomenon has no counterpart in the gas phase, as the orbital remains fully localized. When engaged in ion solvation, the $3a_1$ orbtial is reduced in energy compared to that of the "water-like" molecules, and the splitting is also reduced (see traces c−e), revealing that the occupied electronic structure is more localized on these water molecules. This effect is more pronounced for the Mg^{2+}-coordinated molecules than for Br^- coordination. Similarly, the unoccupied electronic structure is strongly influenced by the presence of ions. The orbitals originating from $4a_1$ give a PDOS that is smooth and broad for "water-like" molecules, with a maximum around 12.5 eV. Upon ion solvation, this state starts to show more structure (compare with the PDOS of the "water-like" molecule)

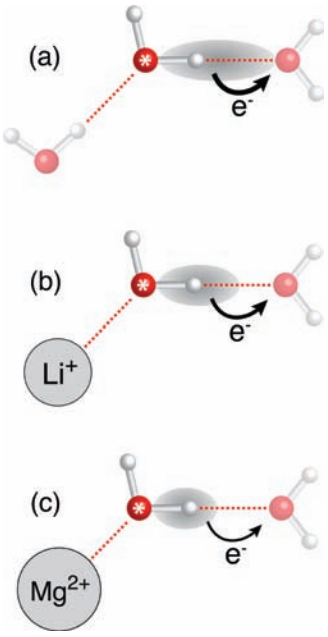

Figure 5. Principle sketch of how we can schematically understand why ions have an effect on the electron-hopping rate in the resonantly excited states of water molecules in aqueous solutions. (a) The situation where a water-coordinated molecule is resonantly excited on the main/post edge. The electron in the excited orbital, which is extended toward the accepting H_2O to the right, can jump to this molecule through its H-donor bond on the time scale of the core-hole decay. (b) The excited molecule is sitting in the first solvation shell of a lithium cation. The excited orbital will then be "back-polarized" toward the parent molecule, and the overlap with the neighboring water molecule on the donor side will be reduced. (c) When going from lithium to Mg^{2+}, this effect is increased, which is consistent with the experimental observations in Figure 2. Note that the cationic core hole on the central O1s atom (denoted by *) also will limit the spatial extension of the excited electron.

and almost breaks up into two discrete bands. Once again, this effect is the most pronounced for Mg^{2+}-coordinated molecules. This resembles the ion-induced effects seen in the XAS of $MgCl_2$ solutions.[45] In order to better understand the connection between XAS and RAS of the current systems, we have calculated XAS from our MD snapshots; the computational methods and detailed results are given in the SI. Briefly, the analysis shows that it is indeed the cationic charge that, to a large extent, causes the increased structuring in the XAS of cation-coordinated water, which here has been shown to result in a reduced electron delocalization dynamics into the H-bonded surroundings.

The reduced electronic mixing with the environment, as observed in both the occupied and unoccupied orbitals for ion-coordinated water molecules, can thus be seen as having two different (but closely related) causes: First, the water−ion bonds perturb the H_2O electronic states and shift them down in energy. This leads to an energetic mismatch with the "water-like" neighbors, which decreases the mixing in the H-bonding between the different class of molecules. Second, the electrostatic interaction between a water molecule and the solvated ions will influence the spatial extension of the orbitals in both the ground and excited states. A core-excited electron of a water molecule (which has high density along the H-donor bond) located in the first solvation shell of a cation will hence be "back-polarized" toward the parent molecule. This effect limits the spatial overlap with the acceptor site (thereby reducing the delocalization rate) and should scale with the charge of the cation, in agreement with the experimental observations in Figure 2. The mechanism is schematically illustrated in Figure 5, where a core-excited water molecule is binding with its oxygen side to (a) another water molecule, (b) Li^+, or (c) Mg^{2+}, resulting in gradually weaker electronic overlap with the right-hand molecule to which it donates a H-bond. Note that the presence of the cationic core hole, which was not taken into account in the PDOS calculations shown in Figure 5 (but in the XAS discussed in the SI), will further increase this effect. Interaction with anions also results in changes in the PDOS of coordinating water molecules, but the effect is less pronounced than for cation coordination, especially in the unoccupied orbitals.

4. CONCLUSIONS

By a combination of O1s resonant Auger spectroscopy and electronic structure calculations of geometries obtained from MD simulations, we have studied the effects of ion solvation on the electron dynamics upon core excitation of water molecules in LiBr and $MgBr_2$ aqueous solutions. The solute-induced changes in the resonant Auger spectra at the main- and post-edge excitations reveal an increased localization of the excited electron in the final states. At the pre-edge, however, the excited electron remains localized both in pure water and in the electrolytes—as a consequence, the Auger spectra are very similar. Using the core-hole clock method, we have determined the electron delocalization times to be ∼1.5 and 1.9 fs upon post-edge excitation in aqueous 6 *m* LiBr and 3 *m* $MgBr_2$, respectively, i.e., up to a 4-fold increase compared to the corresponding value for pure water. Electronic structure calculations have revealed that water molecules engaged in ion solvation show a reduced orbital mixing with the H-bonded surroundings. This effect, which provides a rationalization for the experimental results, has been found to be most pronounced for cation-coordinated molecules and increases with the cationic charge. On the basis of our findings, we have proposed a molecular mechanism in which the excited electron of a core-excited cation-coordinated water is "back-polarized" toward its parent molecule, reducing its propensity to jump through one of its donor H-bonds during the core-hole lifetime.

The present work identifies a sign and charge dependence for the efficiency of electron transfer in aqueous solutions on the direct local environment of the electron-donating water molecules. Such effects may need to be considered in accurate models of charge transfer in strongly perturbed aqueous media, such as intracellular water.

■ ASSOCIATED CONTENT

Supporting Information. Description of model for calculation of changes in electron delocalization times from resonant Auger spectra, details on analysis of MD simulations, description of XAS calculations, and complete ref 40. This material is available free of charge via the Internet http://pubs.acs.org.

■ AUTHOR INFORMATION

Corresponding Author

niklas.ottosson@fysik.uu.se; odelius@fysik.su.se; daniels@mkem.uu.se

■ ACKNOWLEDGMENT

This work was supported by the Knut and Alice Wallenberg foundation, Swedish Scientific Council (VR), The Swedish Foundation for strategic research (SSF), Göran Gustafsson's foundation, Carl Trygger's foundation, and the Magnus Bergvall foundation. We acknowledge generous allocations of computer time through SNIC at the Swedish National Supercomputer Center (NSC) and High Performance Computing Center North (HPC2N), Sweden. B.W. gratefully acknowledges support by the Deutsche Forschungsgemeinschaft (Project WI 1327/3-1).

■ REFERENCES

(1) Atkins, P.; de Paula, J. *Physical Chemistry*; Freeman, W. H., Ed.; OUP: Oxford, 2001.
(2) Marcus, R. A. *J. Chem. Phys.* **1956**, *24*, 966.
(3) Oregan, B.; Gratzel, M. *Nature* **1991**, *353*, 737.
(4) Chen, X.; Bradforth, S. E. *Annu. Rev. Phys. Chem.* **2008**, *59*, 203.
(5) Marx, D.; Tuckerman, M. E.; Hutter, J.; Parrinello, M. *Nature* **1999**, *397*, 601.
(6) Nordlund, D.; Ogasawara, H.; Bluhm, H.; Takahashi, O.; Odelius, M.; Nagasono, M.; Pettersson, L. G. M.; Nilsson, A. *Phys. Rev. Lett.* **2007**, 99.
(7) Björneholm, O.; Nilsson, A.; Sandell, A.; Hernnäs, B.; Mårtensson, N. *Phys. Rev. Lett.* **1992**, *68*, 1892.
(8) Georges, A.; Kotliar, G.; Krauth, W.; Rozenberg, M. J. *Rev. Mod. Phys.* **1996**, *68*, 13.
(9) Winter, B.; Faubel, M. *Chem. Rev.* **2006**, *106*, 1176.
(10) Winter, B. *Nucl. Instrum. Methods A* **2009**, *601*, 139.
(11) Berendsen, H. J. C.; Grigera, J. R.; Straatsma, T. P. *J. Phys. Chem.* **1987**, *91*, 6269.
(12) Horinek, D.; Mamatkulov, S. I.; Netz, R. R. *J. Chem. Phys.* **2009**, *130*, 124507.
(13) Spångberg, D.; Hermansson, K. *J. Chem. Phys.* **2003**, *119*, 7263.
(14) Åqvist, J. *J. Phys. Chem.* **1990**, *94*, 8021.
(15) Perram, J. W.; Petersen, H. G.; Leeuw, S. W. *Mol. Phys.* **1988**, *65*, 875.
(16) Nose, S. *Mol. Phys.* **1984**, *52*, 255.
(17) Hoover, W. G. *Phys. Rev. A* **1985**, *31*, 1695.
(18) Andersen, H. C. *J. Comput. Phys.* **1983**, *52*, 24.
(19) Barth, E.; Kuczera, K.; Leimkuhler, B. J.; Skeel, R. D. *J. Comput. Chem.* **1995**, *16*, 1192.
(20) Swope, W. C.; Andersen, H. C.; Berens, P. H.; Wilson, K. R. *J. Chem. Phys.* **1982**, *76*, 637.
(21) Burgess, J. *Ions in solution*; Ellis Horwood: Chichester, England, 1988.
(22) *CPMD*, V3.11; IBM Corp., 1990−2006; MPI für Festkoerperforschung Stuttgart, 1997−2001.
(23) Cavalleri, M.; Odelius, M.; Nilsson, A.; Pettersson, L. G. M. *J. Chem. Phys.* **2004**, *121*, 10065.
(24) Nordlund, D.; Odelius, M.; Bluhm, H.; Ogasawara, H.; Pettersson, L. G. M.; Nilsson, A. *Chem. Phys. Lett.* **2008**, *460*, 86.
(25) Cavalleri, M.; Odelius, M.; Nordlund, D.; Nilsson, A.; Pettersson, L. G. M. *Phys. Chem. Chem. Phys.* **2005**, *7*, 2854.
(26) Becke, A. D. *Phys. Rev. A* **1988**, *38*, 3098.
(27) Lee, C.; Yang, W.; Parr, R. G. *Phys. Rev. B* **1988**, *37*, 785.
(28) Troullier, N.; Martins, J. L. *Phys. Rev. B* **1991**, *43*, 1993.
(29) Kleinman, L.; Bylander, D. M. *Phys. Rev. Lett.* **1982**, *48*, 1425.
(30) Goedecker, S.; Teter, M.; Hutter, J. *Phys. Rev. B* **1996**, *54*, 1703.
(31) Hartwigsen, C.; Goedecker, S.; Hutter, J. *Phys. Rev. B* **1998**, *58*, 3641.
(32) Odelius, M. *J. Phys. Chem. A* **2009**, *113*, 8176.
(33) Wernet, Ph.; Nordlund, D.; Bergmann, U.; Cavalleri, M.; Odelius, M.; Ogasawara, H.; Näslund, L. Å.; Hirsch, T. K.; Ojamäe, L.; Glatzel, P.; Pettersson, L. G. M.; Nilsson, A. *Science* **2004**, *304* (5673), 995–999.
(34) Winter, B.; Hergenhahn, U.; Faubel, M.; Björneholm, O.; Hertel, I. V. *J. Chem. Phys.* **2007**, *127*, 094501.
(35) Piancastelli, M. N. *J. Electron. Spectrosc. Relat. Phenom.* **2000**, *107*, 1.
(36) Sörensen, S. L.; Svensson, S. *J. Electron. Spectrosc. Relat. Phenom.* **2001**, *114*, 1.
(37) Winter, B.; Aziz, E. F.; Hergenhahn, U.; Faubel., M.; Hertel, I. V. *J. Chem. Phys.* **2007**, *126*, 124504.
(38) Spångberg, D.; Hermansson, K. *J. Chem. Phys.* **2004**, *120*, 4829.
(39) Pokapanich, W.; Ottosson, N.; Svensson, S.; Björneholm, O.; Winter, B.; Öhrwall, G., manuscript submitted, 2011.
(40) Öhrwall, G.; et al. *J. Chem. Phys.* **2005**, *123*, 054310.
(41) Odelius, M.; Cavalleri, M.; Nilsson, A.; Pettersson, L. G. M. *Phys. Rev. B* **2006**, *73*, 024205.
(42) Hüfner, S. *Photoelectron Spectroscopy: Principles and Applications*; Springer: Berlin, 2003.
(43) Wurth, W.; Rocker, G.; Feulner, P.; Scheuerer, R.; Zhu, L.; Menzel, D. *Phys. Rev. B* **1993**, *47*, 6697.
(44) Cappa, C. D.; Smith, J. D.; Wilson, K. R.; Messer, B. M.; Gilles, M. K.; Cohen, R. C.; Saykally, R. J. *J. Phys. Chem. B* **2005**, *109*, 7046.
(45) Cappa, C. D.; Smith, J. D.; Messer, B. M.; Cohen, R. C.; Saykally, R. J. *J. Phys. Chem. B* **2006**, *110*, 5301.
(46) Näslund, L.-Å.; Edwards, D. C.; Wernet, P.; Bergmann, U.; Ogasawara, H.; Pettersson, L. G. M.; Myneni, S.; Nilsson, A. *J. Phys. Chem. A* **2005**, *109*, 5995.
(47) Waluyo, I.; Huang, C.; Nordlund, D.; Bergmann, U.; Weiss, T. M.; Pettersson, L. G. M.; Nilsson, A. *J. Chem. Phys.* **2011**, *134*, 064513.